Investigation for Suitable Target-Projectile Combination for Fusion from the Isotopes of Ti and Nd using Intrinsic Fusion and Fission Barriers Analysis

Dalip Singh Verma[1*] (ID) **Kushmakshi**[1] (ID) **and Monika Manhas**[2] (ID)

[1]*Department of Physics and Astronomical Science, Central University of Himachal Pradesh, Dharamshala, Kangra (H.P.)-176215, India*

[2]*Department of Physics, Government Nehru Degree College, Burhar, Madhya Pradesh − 484001, India*

[*]dsverma@cuhimachal.ac.in (Corresponding Author)

ARTICLE INFORMATION

ABSTRACT

Background: A configuration is most suitable for the fusion if it corresponds to a minimum intrinsic fusion barrier and maximum fission barrier.

Purpose: To find a suitable target-projectile combination from the isotopes of Ti and Nd by analyzing the intrinsic fusion and fission barriers theoretically by including the deformations up to hexadecapole order.

Methods: The fragmentation theory has been used for the calculations.

Results: The intrinsic fusion barrier is minimum and fission barrier is maximum for the target-projectile combination: ^{43}Ti+^{150}Nd in belly-belly configuration, and the inclusion of deformation of higher order leads to the decrease of fission barrier for the prolate shaped cases and compactness for most of the cases.

Conclusions: The most suitable target-projectile combination from the isotopes of Ti and Nd for the fusion is ^{43}Ti+^{150}Nd.

1. Introduction

In deformed heavy-ion collisions the final-state observables as well as properties of the dynamics of the fusion or fusion-fission process is expected to be different from the spherical cases. This is due to the distinct differences in the overlap region of aligned deformed nuclei in the process of fusion and hence an investigation of the shape effects during collisions is important to understand the mechanism and dynamics of the process. The interaction potential is not only the function of the deformations of the interacting nuclei but it also depends on their orientations. The orientation which corresponds to the maximum height of fission barrier V_B and minimum interaction radius R_B is known as hot compact and which gives minimum V_B and maximum R_B is cold elongated [1]. In a recent work of ref. [2] hot compact and cold elongated configurations have been obtained for the isotopes of Ti and Nd, with nuclei oriented at belly-belly (b-b) and tip-tip (t-t) configurations, respectively, with quadrupole deformation only. As the nuclei are not quadrupole deformed only so investigations with respect to the higher deformations will be interesting.

In this paper, we have obtained a suitable target-projectile for the fusion from the various combinations of the deformed and oriented isotopes of Ti and Nd: ^{44}Ti ($\beta_2=\beta_4=0$), ^{43}Ti ($\beta_2=-0.042$, $\beta_4=0.012$), ^{48}Ti ($\beta_2=0.011$; $\beta_4=0$) and ^{142}Nd ($\beta_2=\beta_4=0$), ^{181}Nd ($\beta_2=-0.125$; $\beta_4=−0.006$) and ^{150}Nd ($\beta_2=0.237$; $\beta_4=0.110$) by investigating the V_B and R_B for the b-b and t-t configurations, and intrinsic fusion barrier $B_{fus,}$ in mass asymmetric coordinates, for b-b configuration only due to lesser values of V_B for t-t configuration. It may be noted that $\beta_3=0$ for these nuclei and the deformation values are of ref. [3]. These barriers play an important role in understanding the competition between quasi-fission and complete fusion. Following the definition of B_{fus} in charge asymmetry coordinate of ref. [4], B_{fus} in mass asymmetry coordinate is defined as the height of the saddle point (the maximum fragmentation potential) from the potential which corresponds to the incoming channel mass asymmetry or mass number of the projectile. The smaller value of B_{fus} favours complete fusion while the larger value of it is a hindrance to the fusion process.

In the following we discussed the methodology, calculations and results, and conclusion of the study.

2. Methodology

The fragmentation theory [5, 6] used to obtain the fragmentation potentials is worked out in terms of mass asymmetry coordinate $\eta = (A_1 - A_2)/(A_1 + A_2)$ or charge asymmetry coordinate $\eta_Z = (Z_1 - Z_2)/(Z_1 + Z_2)$, relative separation R, the neck-length parameter ε and the deformations of the interacting nuclei $\beta_{\lambda i}$ (i = 1, 2 and λ = 2, 3, 4 for the quadrupole, octupole, and hexadecapole deformations). According to the fragmentation theory the fragmentation potential between two deformed and oriented nuclei colliding in a plane (ϕ = 0) at fixed inter-nuclear separation R_a is

$$V(\eta, \eta_Z, R) = \sum_{i=1}^{2} V_{LDM}(A_i, Z_i)$$
$$+ \sum_{i=1}^{2} \delta U_i + V_P(R, A_i, \beta_{\lambda i}, \theta_i, \varphi) \quad (1)$$
$$+ V_C(R, Z_i, \beta_{\lambda i}, \theta_i, \varphi)$$
$$+ V_\ell(R, A_i, \beta_{\lambda i}, \theta_i, \varphi)$$

where $V_{LDM}(A_i, Z_i)$, δU_i, V_P, V_C and V_ℓ respectively are the liquid drop energies, shell corrections, proximity potential, Coulomb potential and centrifugal potential between the fragments. For a given nucleus $V_{LDM}(A, Z)$ [7] is

$$V_{LDM}(A, Z) = \alpha A + \beta A^{2/3} + \left(\gamma - \frac{\eta}{A^{1/3}}\right)\left|\frac{4t_\zeta^2 - 4|t_\zeta|}{A}\right|$$
$$+ \frac{Z^2}{R_0 A^{1/3}}\left(1 - \frac{0.7636}{Z^{2/3}} - \frac{2.29}{\left(R_0 A^{1/3}\right)^2}\right) \quad (2)$$
$$+ \delta\left(\frac{f(Z, A)}{A^{3/4}}\right)$$

where α, β, γ, η and a_a are Seeger's constants [8], $t_\zeta = a_a(Z - N)$ is the asymmetry term and a_a is the asymmetry constant. The shell correction δU for a given nucleus is taken from [9]. The bulk α and asymmetry a_a constants are obtained by equating the ground state mass excess of AME2016 [10] or of FRDM(2012) [3] by with $V_{LDM}(A, Z) + \delta U$ [11]. The Coulomb and proximity potentials for deformed and oriented nuclei for ϕ = 0 are given as:

$$V_c(R, Z_i, \beta_{\lambda i}, \theta_i) = \frac{Z_1 Z_2 e^2}{R}$$
$$+ \sum_{\lambda, i=1,2} \frac{3 Z_1 Z_2 e^2}{2\lambda + 1} \frac{R_i^\lambda(\alpha_i)}{R^{\lambda+1}} Y_\lambda^{(0)}(\theta_i) \quad (3)$$
$$\times\left[\beta_{\lambda i} + \frac{4}{7}\beta_{\lambda i}^2 Y_\lambda^{(0)}(\theta_i)\right]$$

$$V_P(R, A_i, \beta_{\lambda i}, \theta_i) = 4\pi \bar{R} \gamma b \Phi(s_0) \quad (4)$$

where $\gamma = 0.9517[1 - 1.7826((N-Z)/A)^2]$ MeV fm^{-2} is the nuclear surface energy constant, b (= 0.99 fm) is the nuclear surface thickness and $\Phi(s_0)$ is the universal function, given as

$$\Phi(s_0) = \begin{cases} -0.5(s_0 - 2.54)^2 - 0.0852(s_0 - 2.54)^3 & \text{for } s_0 \leq 1.2511 \\ -3.437\exp(-s_0/0.75) & \text{for } s_0 \geq 1.2511 \end{cases}$$
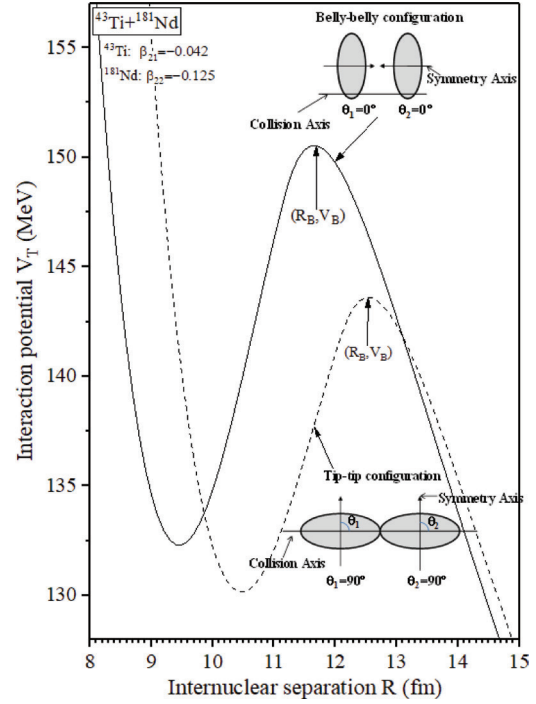$$(5)$$

Figure 1: Interaction potential for tip-tip and belly-belly configurations of the oblate shaped P-T.

where s_0 is the minimum separation between the surfaces of the interacting nuclei per unit surface thickness. The mean curvature radius $\bar{R}$ for axially symmetric deformed and oriented nuclei is of ref. [12]. The separation between the surfaces of two interacting nuclei is, $s_0 = R - R_1(\alpha_1)\cos(\theta_1 - \alpha_1) - R_2(\alpha_2)\cos(180 + \theta_2 - \alpha_2)$ and become minimum when $ds_0/d\alpha_1 = ds_0/d\alpha_2 = 0$ (for detail see [1, 13] and references therein). The scattering/interaction potential between the two interacting nuclei V(R) is the sum of the proximity potential V_P and Coulomb potential V_C, i.e., $V_T(R) = V_P(R) + V_C(R)$ for ℓ=0 case.

3. Calculations and Results

Fig. 1 shows the interaction potential for the oblate shaped projectile-target combination ^{43}Ti+^{181}Nd oriented at (0°, 0°)

for hot and (90°, 90°) for cold configurations called belly-belly and tip-tip configurations, respectively. The barrier height (V_B) is maximum and interaction radius (R_B) is minimum for the belly-belly configuration while for the tip-tip configuration corresponds to the minimum of V_B and maximum of R_B, whatever may be the sign of the deformation.

This has been explored for various combinations of Ti and Nd: oblate-oblate, oblate-prolate, oblate-spherical, prolate-oblate, prolate-prolate, prolate-spherical, spherical-oblate and spherical-prolate, as tabulated in Table: 1 and 2 below along with the inclusion of deformation of higher order (±).

Table 1: P-T oriented for belly-belly (b-b) configuration (Hot fusion).

S. N.	P-T (b-b configurations)	P-T Orientation (θ_1, θ_2)	P-T with β_{2i} (i=1,2)	V_B (MeV)	R_B (fm)	P-T with $\beta_{2i}+\beta_{3i}+\beta_{4i}$ (i=1,2)	V_B (MeV)	R_B (fm)
1.	^{43}Ti+^{181}Nd	(0°, 0°)	o − o	148.79	11.80	o$^+$ − o$^-$	148.79	12.50
2.	^{43}Ti+^{150}Nd	(0°, 90°)	o − p	154.19	11.36	o$^+$- p$^+$	152.96	11.46
3.	^{43}Ti+^{142}Nd	(0°, 0°)	o − s	152.60	11.60	o − s	152.60	11.70
4.	^{48}Ti+^{181}Nd	(90°, 0°)	p − o	146.77	11.97	p − o$^-$	146.77	11.97
5.	^{48}Ti+^{150}Nd	(90°, 90°)	p − p	151.46	11.58	p − p$^+$	151.00	11.60
6.	^{48}Ti+^{142}Nd	(90°, 0°)	p − s	149.69	11.86	p − s	149.69	11.91
7.	^{44}Ti+^{181}Nd	(0°, 0°)	s − o	147.99	11.90	s − o$^-$	147.99	12.60
8.	^{44}Ti+^{150}Nd	(0°, 90°)	s − p	153.01	11.48	s − p$^+$	151.80	11.58

Table 2: P-T oriented for tip-tip (t-t) configuration (Cold fusion).

S. N.	P-T (t-t configurations)	P-T Orientation (θ_1, θ_2)	P-T with β_{2i} (i=1,2)	V_B (MeV)	R_B (fm)	P-T with $\beta_{2i}+\beta_{3i}+\beta_{4i}$ (i=1,2)	V_B (MeV)	R_B (fm)
1.	^{43}Ti+^{181}Nd	(90°, 90°)	o − o	142.41	12.50	o$^+$ − o$^-$	142.41	12.50
2.	^{43}Ti+^{150}Nd	(90°, 0°)	o − p	142.07	12.80	o$^+$- p$^+$	136.86	13.30
3.	^{43}Ti+^{142}Nd	(90°, 0°)	o − s	151.28	11.70	o − s	151.28	11.70
4.	^{48}Ti+^{181}Nd	(0°, 90°)	p − o	140.69	12.80	p − o$^-$	140.69	12.80
5.	^{48}Ti+^{150}Nd	(0°, 0°)	p − p	140.45	13.00	p − p$^+$	136.07	13.40
6.	^{48}Ti+^{142}Nd	(0°, 0°)	p − s	149.35	11.91	p − s	149.35	11.91
7.	^{44}Ti+^{181}Nd	(0°, 90°)	s − o	142.24	12.60	s − o$^-$	142.24	12.60
8.	^{44}Ti+^{150}Nd	(0°, 0°)	s − p	142.14	12.80	s − p$^+$	136.99	13.30

It can be seen from Table 1 and 2 that the V_B is maximum and R_B is minimum for the reaction ^{43}Ti+^{150}Nd in belly-belly configuration, and hence is predicted to be the best target-projectile for fusion. The addition of higher order deformation leads to the decrease of height of fission barrier (V_B) in p$^+$ (prolate with β_4=+ve) cases and increase of the interaction radius in most of the cases. This means that the systems become less compact with the inclusion of deformation of higher order and compact configuration is expected to be at some other orientation, as can be seen in ref. [14].

Thus a configuration of compactness is most suitable for the fusion process. The suitability is explored further in terms of B_{fus}. It may be noted that the inclusion of the deformations of higher order (±) does not change the optimal orientation, but leads to a decrease in the compactness.

Fig. 2 illustrate the intrinsic fusion barrier B_{fus} for ^{43}Ti+^{181}Nd reaction when target and projectile considered are: (i) spherical, (ii) quadrupole deformed (β_{2i}) and (iii) with deformation of higher order such as octupole (β_{3i}) and hexadecapole (β_{4i}) i.e., p$^\pm$, o$^\pm$. The intrinsic fusion barrier B_{fus} increases with the inclusion of the deformation of higher order, i.e., $B_{fus}(\beta_{2i}) < B_{fus}(\beta_{2i} + \beta_{3i} + \beta_{4i})$, which seems to be due to the decrease of the compactness with the higher deformations [14].

Table 3 clearly shows that for $^{43}\text{Ti}+^{150}\text{Nd}\rightarrow^{193}\text{Pb}^*$ the intrinsic fusion barrier B_{fus} is zero when target and projectiles are considered quadrupole deformed (β_{2i}) and is minimum (=0.84 MeV) when the deformations of

higher orders (β_{3i} and β_{4i}) are included. Thus $^{43}\text{Ti}+^{150}\text{Nd}$ reaction or target-projectile combination seems to be the best for the fusion when oriented at belly-belly configuration.

Table 3: Intrinsic fusion barriers for hot optimum or belly-belly Configuration.

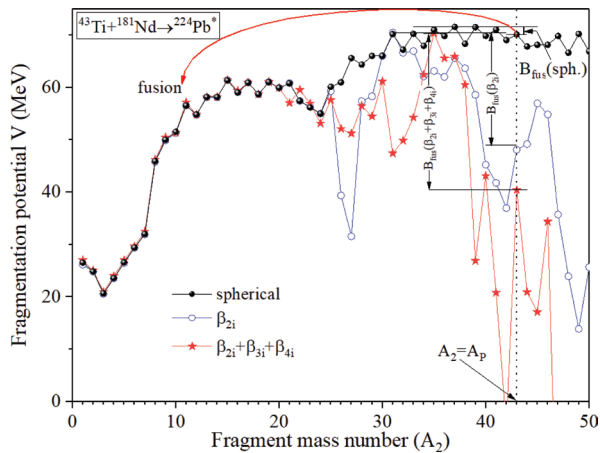| S. N.	P-T (b-b configurations)	P-T with β_{2i} (i=1,2)	B_{fus} (MeV)	P-T with $\beta_{2i}+\beta_{3i}+\beta_{4i}$ (i=1,2)	B_{fus} (MeV)
1.	$^{43}\text{Ti}+^{181}\text{Nd}\rightarrow^{224}\text{Pb}^*$	o − o	22.39	$o^+ - o^-$	29.94
2.	$^{43}\text{Ti}+^{150}\text{Nd}\rightarrow^{193}\text{Pb}^*$	o − p	0	$o^+ - p^+$	0.84
3.	$^{43}\text{Ti}+^{142}\text{Nd}\rightarrow^{185}\text{Pb}^*$	o − s	0.75	o − s	6.39
4.	$^{48}\text{Ti}+^{181}\text{Nd}\rightarrow^{229}\text{Pb}^*$	p − o	43.44	$p - o^-$	152.51
5.	$^{48}\text{Ti}+^{150}\text{Nd}\rightarrow^{198}\text{Pb}^*$	p − p	5.71	$p - p^+$	47.70
6.	$^{48}\text{Ti}+^{142}\text{Nd}\rightarrow^{190}\text{Pb}^*$	p − s	8.64	p − s	148.15
7.	$^{44}\text{Ti}+^{181}\text{Nd}\rightarrow^{225}\text{Pb}^*$	s − o	18.83	$s - o^-$	48.42
8.	$^{44}\text{Ti}+^{150}\text{Nd}\rightarrow^{194}\text{Pb}^*$	s − p	4.95	$s - p^+$	26.63

Figure 2: Fragmentation potential illustrating intrinsic fusion barrier B_{fus} for (i) spherical and deformed with (ii) β_{2i} and (iii) $\beta_{2i}+\beta_{3i}+\beta_{4i}$.

Conclusions

An analysis of intrinsic fusion barrier, fission barrier height and position reveals that the most compact orientation (belly-belly) of the colliding nuclei seems to be the best for the fusion of heavy-ions and can be obtained using the barrier analysis, here predicting $^{43}\text{Ti}+^{150}\text{Nd}$ as the best target-projectile combination for the synthesis of Pb.

Acknowledgements

Authorship Contribution

Conception of the idea, interpretation of the data/results and manuscript preparation by Dalip Singh Verma, running codes, extracting the data for figures by Kushmakshi, and manuscript preparation and interpretation of the results by Monika Manhas. All authors discussed the results and contributed to the final manuscript.

Funding

Conflict of Interest

There is no conflict of interests.

Declaration

It is declared that the results presented in this paper are original and has neither been sent elsewhere, nor published anywhere.

References

[1] R. K. Gupta, M Balasubramaniam, R. Kumar, *et al.*, J. Phys. G: Nucl. Part. Phys. **31**, 631 (2005). https://doi.org/10.1088/0954-3899/31/7/009

[2] H. Sharma and D. S. Verma, DAE Symp. on Nucl. Phys. **63,** 494-495 (2005).

[3] P. Möller, A.J. Sierk, T. Ichikawa, *et al.*, Atomic and Nuclear Data Table **109-110**, 1-204 (2016).
https://doi.org/10.1016/j.adt.2015.10.002

[4] A. Nasirov, A. Fukushima, Y. Toyoshima, *et al.*, Nucl. Phys. A **759**, 342-369 (2005).
https://doi.org/10.1016/j.nuclphysa.2005.05.152

[5] A. Săndulescu, R. K. Gupta, W. Scheid, W. Greiner, Phys Lett. B **60 (3**), 225-228 (1976).
https://doi.org/10.1016/0370-2693(76)90286-0

[6] R. K. Gupta, M. Balasubramaniam, G. Münzenberg, *et al.*, J Phys G: Nucl Part Phys **27**, 867-881 (2001).
https://doi.org/10.1088/0954-3899/27/4/31

[7] N. J. Davidson, S. S. Hsiao, J. Markram, H. G. Miller, Y. Tzeng, Nucl Phys A **570** c 61-68 (1994).
https://doi.org/10.1016/0375-9474(94)90269-0

[8] P. A. Seeger, Nucl. Phys. **25**, 1–135 (1961).
https://doi.org/10.1016/0029-5582(61)90147-X

[9] W. D. Myers, W. J. Swiatecki, Nucl Phys **81**, 1-60 (1966).
https://doi.org/10.1016/0029-5582(61)90147-X

[10] M. Wang, G. Audi, F.G. Kondev, *et al.*, Chin.Phys **C 41,** 030003 (2017).
https://doi.org/10.1088/1674-1137/41/3/030003

[11] D. S. Verma and Kushmakshi, J. Radioanal. Nucl. Chem. **322**, 139–146 (2019).
https://doi.org/10.1007/s10967-019-06497-7

[12] J. Blocki, J. Randrup, W. J. Swiatecki and C. F. Tsang, Ann. Phys. **105**, 427–462 (1977).
https://doi.org/10.1016/0003-4916(77)90249-4

[13] R. K. Gupta, N. Singh, and M. Manhas, Phys. Rev. C **70**, 034608 (2004).
https://doi.org/10.1103/PhysRevC.70.034608

[14] R. K. Gupta, M. Manhas, and W. Greiner, Phys. Rev. C **73**, 054307 (2006).
https://doi.org/10.1103/PhysRevC.73.054307